Journal of Physics: Conference Series **303** (2011) 012037 doi:10.1088/1742-6596/303/1/012037

Octacyanoniobate(IV)-based molecular magnets revealing 3D long-range order

R Pełka[1], D Pinkowicz[2], O Drath[2], M Bałanda[1], M Rams[3], A Majcher[3], W Nitek[2] and B Sieklucka[2]

[1] Institute of Physics PAN, Radzikowskiego 152, 31-342, Kraków, Poland
[2] Faculty of Chemistry, Jagiellonian University, Ingardena 3, 30-060 Kraków, Poland
[3] Institute of Physics, Jagiellonian University, Reymonta 4, 30-059 Kraków, Poland

robert.pelka@ifj.edu.pl

Abstract. Isostructural series of chemical formula $\{[M^{II}(pirazol)_4]_2[Nb^{IV}(CN)_8]\cdot 4H_2O\}_n$ (M^{II}=Mn (**1**), Fe (**2**), Co (**3**), Ni (**4**)) has been obtained by the self-assembly technique. Its unique crystallographic structure consists in the formation of a 3D extended network of magnetic centers braced by geometrically identical cyanido bridges. Magnetic measurements reveal the transitions to the 3D order at temperatures 23.7, 8.3, 5.9, 13.4 K for **1**, **2**, **3**, and **4**, respectively. The character of order is demonstrated to be ferrimagnetic for **1** and **2** and ferromagnetic for **3** and **4**. The mean-field approach is used to determine the corresponding exchange coupling constants. The observed interactions are discussed within the magnetic orbital model.

1. Introduction

The field of molecular magnetism has been attracting attention of physicist as a potential source of materials to be used in memory storage devices, magnetic sensors or switches, etc., ever since the first successful synthesis of two magnetic molecular compounds in 1986 [1]. Until present a vast number of molecule-based magnets displaying a striking variety of structural topologies and technologically relevant properties have been reported [2]. Among them a prominent position is taken by those based on cyanido-bridges linking the transition metal ions which are known to display a wide spectrum of structures and functionalities [3]. This rich family of compounds has recently been joined by four 3D isostructural compounds $\{[M^{II}(pyrazole)_4]_2[Nb^{IV}(CN)_8]\cdot 4H_2O\}_n$, where M^{II} = Mn, Fe, Co, Ni, obtained by self assembly of $[Nb^{IV}(CN)_8]^{4-}$ with different 3*d*-metal centers in aqueous solution and excess of pyrazole [4]. All four coordination polymers crystallize in the same I $4_1/a$ space group, see [4] for crystallographic details. Due to specific symmetry of the crystal lattice the M^{II}-NC-Nb^{IV} linkages providing the main exchange coupling pathways between metal centers are geometrically equivalent, which implies a single exchange coupling constant J_{MNb}. The present contribution shows two simple approaches based on the mean-field theory employed to estimate the values of J_{MNb} for **1**-**4**. To this end three magnetic properties have been measured using 7227 Lakeshore AC Susceptometer/DC Magnetometer (**1**, **3**, **4**) or S600X SQUID Magnetometer (**2**): dc susceptibility, isothermal magnetization and thermal dependence of magnetization. The magnetic susceptibility data were corrected for

the diamagnetic contribution using Pascal constants [5]. Isothermal magnetization curves in the field up to 56/50 kOe were measured at T=4.3 K for **1**, **3,** and **4** and at T=2 K for **2**.

2. Theoretical background

The first approach consists in analyzing the thermal dependence of magnetization for **1**, **2**, **3**, and **4**. The calculations follow the lines reported in [6]. The mean field model consists of two sublattices, one sublattice for the Nb^{IV} centers and the other formed by the M^{II} ions. Next, only the superexchange coupling between the nearest-neighbor sites is taken into account. The thermally averaged values of the sublattice spins are given by the following set of coupled equations

$$\langle S_{\mathrm{M}} \rangle = S_{\mathrm{M0}} B_{S_{\mathrm{M0}}} \left(\frac{g_{\mathrm{M}} \mu_B S_{\mathrm{M0}} H_0}{k_B T} + \frac{Z_{\mathrm{MNb}} J_{\mathrm{MNb}} S_{\mathrm{M0}}}{k_B T} \langle S_{\mathrm{Nb}} \rangle \right) \quad (1)$$

$$\langle S_{\mathrm{Nb}} \rangle = S_{\mathrm{Nb0}} B_{S_{\mathrm{Nb0}}} \left(\frac{g_{\mathrm{Nb}} \mu_B S_{\mathrm{Nb0}} H_0}{k_B T} + \frac{Z_{\mathrm{NbM}} J_{\mathrm{MNb}} S_{\mathrm{Nb0}}}{k_B T} \langle S_{\mathrm{M}} \rangle \right) \quad (2)$$

where B_S is the Brillouin function, S_{M0} and S_{Nb0} are the values of $\langle S_{\mathrm{M}} \rangle$ and $\langle S_{\mathrm{Nb}} \rangle$ at $T = 0$ K, k_B is the Boltzmann constant, μ_B is the Bohr magneton, H_0 is the external magnetic field, Z_{ij} are the numbers of the nearest-neighbor j-site ions surrounding an i-site ion, and g_{M} and g_{Nb} are the spectroscopic factors. The total molar magnetization is $M_{\mathrm{total}}=N_A\mu_B[2g_{\mathrm{M}}\langle S_{\mathrm{M}}\rangle+g_{\mathrm{Nb}}\langle S_{\mathrm{Nb}}\rangle]$, where the means $\langle S_{\mathrm{M}} \rangle$ and $\langle S_{\mathrm{Nb}} \rangle$ differ in sign for antiferromagnetic coupling between the M^{II} and Nb^{IV} centers. The numbers of the nearest neighbors are Z_{MNb}=4, Z_{NbM}=2, and we assume S_{Nb0}=1/2, g_{Nb}=2.0. The spin quantum number S_{M0} of the M^{II} center and the corresponding spectroscopic factor g_{M} are case-dependent. The crucial point in the first approach is that the mean-field curve is chosen so that the corresponding peak of the derivative dM/dT coincides with that obtained on the basis of the measured magnetization values. The error of J_{MNb} thus obtained is estimated assuming the uncertainty of 0.5 K in the peak position defining the transition temperature. The calculated mean-field curves display generally higher values of magnetization at low temperatures. This is due to the fact that the calculated magnetizations are essentially the saturated values, because the molecular-field theory does not account for the complex ordering process involving domain formation. Figures 2, 4, 6, and 8 show thermal dependence of magnetization for **1**, **2**, **3**, and **4**, respectively, measured in the external magnetic field H_0=0.5 kOe. The solid lines show the corresponding mean field curves. Inserts of these figures show the derivative dM/dT used to pinpoint the corresponding exchange coupling constants J_{MNb}.

The second approach is based on the mean-field prediction for the magnetic susceptibility at high temperatures which reads

$$\chi = \frac{(2C_{S_{\mathrm{M0}}} + C_{S_{\mathrm{Nb0}}})T + 4\lambda_{\mathrm{MNb}} C_{S_{\mathrm{M0}}} C_{S_{\mathrm{Nb0}}}}{T^2 - 2\lambda_{\mathrm{MNb}}^2 C_{S_{\mathrm{M0}}} C_{S_{\mathrm{Nb0}}}} \quad (3)$$

where $C_S=N_A g^2 \mu_B{}^2 S(S+1)/(3k_B)$ denotes the Curie constant for the corresponding spins, and λ_{MNb} is the molecular field constant. This high-temperature law is a counterpart of the Curie-Weiss law for unequal occupation numbers of the constituent magnetic sublattices. The positive (negative) sign of the molecular field constant corresponds to (anti)ferromagnetic character of the coupling. The exchange coupling constants are calculated from the relation $\lambda_{\mathrm{MNb}}=2J_{\mathrm{MNb}}/(N_A g_{\mathrm{av}}{}^2 \mu_B{}^2)$.

3. Results

3.1. $\{[Mn^{II}(pirazol)_4]_2[Nb^{IV}(CN)_8] \cdot 4H_2O\}_n$

Figure 1 shows the temperature variation of the inverse dc susceptibility for **1**. The fit to the mean-field prediction given by equation (3) in the range of 240-300 K yielded λ_{MnNb}=-28(4) mol cm^{-3} and g_{Mn}=1.99(1). The sign of the molecular-field constant indicates that the manganese and niobium sublattices are coupled antiferromagnetically. This is consistent with the magnetization detected at T=4.3 K (insert of figure 1) saturating at the value of 8.95 ($\approx 2g_{\mathrm{Mn}}S_{\mathrm{Mn0}}$-$g_{\mathrm{Nb}}S_{\mathrm{Nb0}}$=9) μ_{B}. The calculated

mean-field $M(T)$ curve (figure 2, solid line) assuming the antiferromagnetic interaction between Mn^{II} and Nb^{IV} sublattices yielded J_{MnNb} = -6.8(2) cm^{-1}.

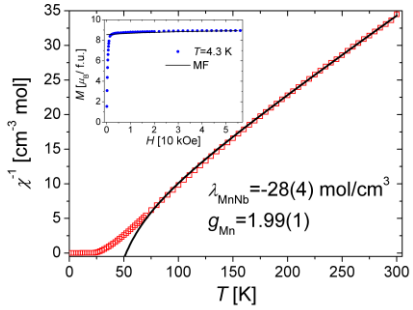

Figure 1. χ^{-1} vs. T for **1**. Solid line - fit to equation (3). Insert: M vs. H at T= 4.3 K.

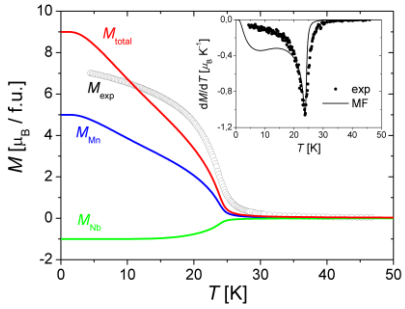

Figure 2. M vs. T obtained in H_{DC} = 0.5 kOe for **1**. Solid lines – the mean-field curves. Insert: dM/dT vs. T used to determine J_{MnNb}.

3.2. $\{[Fe^{II}(pirazol)_4]_2[Nb^{IV}(CN)_8]\cdot 4H_2O\}_n$

Figure 3 shows the inverse of the dc susceptibility for **2**. The fit to equation (3) in the temperature range 150-300 K yielded λ_{FeNb}=+16.2(3) mol/cm^3 and g_{Fe}=2.163(2) [7]. The isothermal magnetization measured at T=2 K (insert of figure 3) shows a rapid increase followed by a steady linear grow for higher fields. In the field of 50 kOe the magnetization attains the value of 7 μ_B, which is substantially lower than that expected for the ferromagnetic coupling between the Fe^{II} and Nb^{IV} ions ($2g_{Fe}S_{Fe0}+g_{Nb}S_{Nb0}$=9.6), and comparable to that for the antiferromagnetic coupling ($2g_{Fe}S_{Fe0}$-$g_{Nb}S_{Nb0}$=7.6). The deviation of the measured magnetization values from those obtained within the mean-field model as well as the shape of the magnetization curve imply the presence of local anisotropy of the Fe^{II} ions and/or noncollinearity of the constituent magnetic moments. The calculated mean-field $M(T)$ curve (figure 4, solid line) assuming the antiferromagnetic interaction between Fe^{II} and Nb^{IV} sublattices yielded J_{FeNb} = -3.1(2) cm^{-1}.

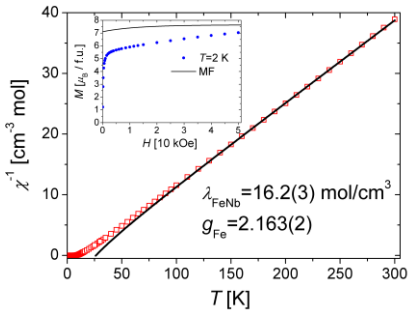

Figure 3. χ^{-1} vs. T for **2**. Solid line - fit to equation (3). Insert: M vs. H at T= 2 K.

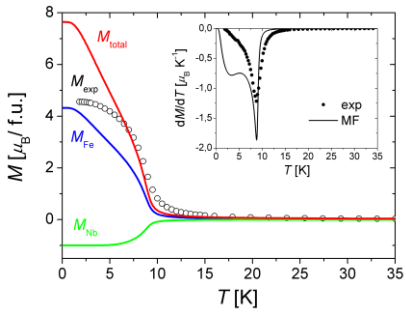

Figure 4. M vs. T obtained in H_{DC} = 0.5 kOe for **2**. Solid lines – the mean-field curves. Insert: dM/dT vs. T used to determine J_{FeNb}.

3.3. $\{[Co^{II}(pirazol)_4]_2[Nb^{IV}(CN)_8]\cdot 4H_2O\}_n$

Isothermal magnetization measured at T=4.3 K for **3** (insert of figure 5) attains the value of 5.55 μ_B in the field of 50 kOe , which indicates that the Co^{II} ion ($3d^7$) must be in the high spin state $(t_{2g})^5(e_g)^2$. In such a case the orbital contribution to the magnetic moment cannot be neglected [8] and a special treatment is necessary. It can be shown (see [4] for more detail) that in octahedral ligand field the ground state of the Co^{II} ion may be described by an effective spin Σ_{Co}=1/2 with Landé factor g_{Co}=13/3≈4.33. Moreover, due to the orbital contribution the exchange coupling should be rescaled by

factor 5/3 [9]. Figure 5 shows the thermal variation of the inverse susceptibility for **3**. Fit to equation (3) in the temperature range 150-300 K implies λ_{CoNb}=+15(1) mol/cm^3 and g_{Co}=4.55(5), which indicates the ferromagnetic coupling between the Co^{II} and Nb^{IV} sublattices. This is consistent with the value of magnetization attained in 50 kOe (5.55 μ_B) as the expected value is $2g_{Co}\Sigma_{Co}+g_{Nb}S_{Nb}$=5.33 μ_B. The calculated mean-field $M(T)$ curve (figure 6, solid line) assuming the ferromagnetic interaction between Co^{II} and Nb^{IV} sublattices yielded J_{CoNb} = +3.5(3) cm^{-1}.

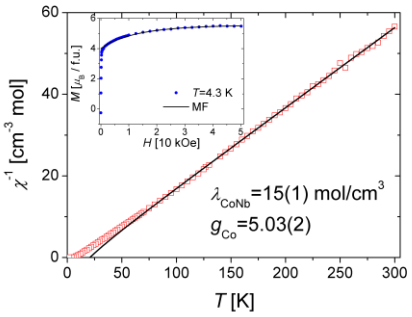

Figure 5. χ^{-1} vs. T for **3**. Solid line - fit to equation (3). Insert: M vs. H at T= 4.3 K.

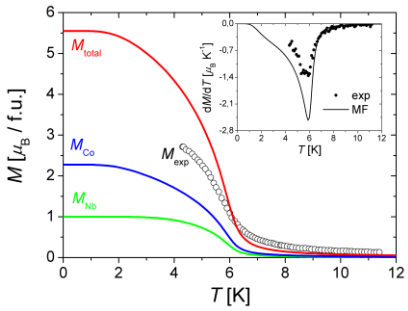

Figure 6. M vs. T obtained in H_{DC} = 0.5 kOe for **3**. Solid lines – the mean-field curves. Insert: dM/dT vs. T used to determine J_{CoNb}.

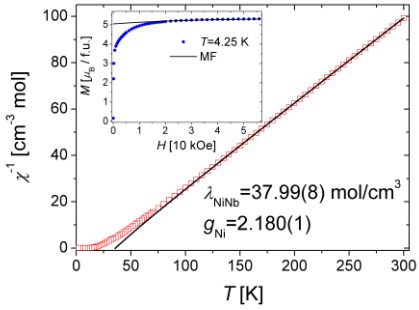

Figure 7. χ^{-1} vs. T for **4**. Solid line - fit to equation (3). Insert: M vs. H at T= 4.25 K.

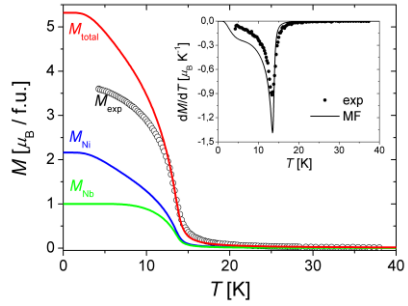

Figure 8. M vs. T obtained in H_{DC} = 0.5 kOe for **4**. Solid lines – the mean-field curves. Insert: dM/dT vs. T used to determine J_{NiNb}.

3.4. $\{[Ni^{II}(pirazol)_4]_2[Nb^{IV}(CN)_8]\cdot 4H_2O\}_n$

For the Ni^{II} ion (3d^8) placed in the octahedral ligand field the orbital degeneracy of the corresponding ground term ^3F (L=3, S=1) is partially lifted and the term splits into two triplets Γ_4 ($^3T_{1g}$) and Γ_5 ($^3T_{2g}$), and a singlet Γ_2 ($^3A_{2g}$) [9], of which the orbital singlet is the lowest lying level. Hence the quantum state of the Ni^{II} is described by spin quantum number S_{Ni0}=1. Due to the spin-orbit interaction, which couples the ground orbital singlet with the triplet Γ_5, one can expect the enhancement of the mean spectroscopic factor for the Ni^{II} g_{Ni}>2.0. Fitting equation (3) in the temperature range 150-300 K (see figure 7) yielded λ_{NiNb}=+37.99(8) mol/cm^3, g_{Ni}=2.180(1), which implies the ferromagnetic coupling between the Ni^{II} and Nb^{IV} sublattices. Insert of figure 7 shows the relatively rapid saturation of magnetization detected at T=4.25 K. The magnetization in H=56 kOe attains the value of 5.31 μ_B, which is consistent with the expected value of $2g_{Ni}S_{Ni0}+g_{Nb}S_{Nb0}$=5.36 μ_B. The calculated mean-field $M(T)$ curve (figure 8, solid line) assuming the ferromagnetic interaction between Ni^{II} and Nb^{IV} sublattices yielded J_{NiNb} = +8.1(3) cm^{-1}.

4. Discussion

Table 1 recapitulates the results obtained for compounds **1**-**4**. Two last columns list the exchange coupling constants J_{MNb} obtained from the adjustment of the dM/dT peak and on the basis of the molecular-field constant λ_{MNb}. It can be seen that the values obtained by the latter approach are consistently higher than those given by the former one. These differences may originate from the fact that the mean-field model overestimates the transition temperature and hence the lower values for J_{MNb} obtained on the basis of the dM/dT peak position. For **2** the positive sign of λ_{FeNb} is inconsistent with antiferromagnetic character of exchange coupling implied strongly by low magnetization values, which suggests that the fits to equation (3) may not always be reliable. Therefore in further discussion we will refer to the exchange couplings determined by the former approach.

Table 1. Parameters of the mean-field calculation for **1**-**4**.

No.	M^{II}	Coupling assumed	S_{M0}	T_c [K]	g_M	λ_{MNb} [mol cm^{-3}]	J_{MNb} [cm^{-1}] dM/dT peak	J_{MNb} [cm^{-1}] from λ_{MNb}
1	Mn	AF	5/2	23.7(5)	1.99(1)	-28(4)	-6.8(2)	-14(2)
2	Fe	AF	2	8.3(5)	2.163(2)	+16.2(3)	-3.1(2)	+9.1(2)
3	Co	F	1/2	5.9(5)	4.55(5)	+15(1)	+3.5(3)	+11.8(8)
4	Ni	F	1	13.4(5)	2.180(1)	+37.99(8)	+8.1(3)	+21.6(1)

The values of exchange couplings found for **1**, **2**, **3**, and **4** indicate the presence of antiferromagnetic pathways within the Nb^{IV}-CN-M^{II} unit. They are expected to arise due to a "through bond" interaction, i.e. the overlap between the magnetic orbital centered on the $4d_{x2-y2}$ orbital of niobium (the lowest state for the DD coordination geometry) and some of the 3d orbitals of the metal ion. The monotonic increase of exchange constants $J_{MnNb}<J_{FeNb}<0<J_{CoNb}<J_{NiNb}$ revealed consistently by both approaches points out that the ferromagnetic terms contributing to the total exchange constant arising from the orthogonality of the $4d_{x2-y2}$ niobium orbital with some of the M^{II}-centered orbitals may not be negligible, despite the fact that the Nb^{IV} ion and the M^{II} ion is located at the sizable distance of about 5.6 Å. There is an evident correlation between the decreasing number of singly occupied 3d orbitals on the M^{II} ion (5, 4, 3, and 2 for **1**, **2**, **3** and **4** respectively) and the increasing trend in the exchange coupling constant. For the DD geometry, the $4d_{x2-y2}$ orbital of the Nb^{IV} ion is σ nonbonding because all the ligand atoms are located in the nodal planes of this orbital [10]. On the other hand, the lowest d level substantially mixes with the π system of the cyanido ligands. It was shown [10] that the overlap between the d_{x2-y2} orbital and the π orbital of the ligand orthogonal to the nodal plane in which the ligand is located is more efficient for the ligands on the vertexes with θ=69.46° than those on the vertexes with θ=36.85°. As for all the compounds the bridging ligands are located on the former vertexes, one can expect a relatively stronger exchange coupling. Among the magnetic orbitals (singly occupied molecular orbitals) centered on the partially occupied orbitals of the M^{II} ion, there are two of the t_{2g} type (d_{xy}, d_{xz}) which can be expected to be effectively delocalized on the nitrogen and the carbon of the cyanido group (π symmetry). Even for the remaining t_{2g} orbital (d_{yz}) a weak overlap with the orbitals centered on the bridging cyanido group can be expected due to its bending. At the same time, the magnetic orbital centered on the $4d_{x2-y2}$ orbital of Nb^{IV} is also partially delocalized on the carbon and nitrogen (with the same π symmetry) of the cyanido group. For two electrons, we can apply the Kahn's model ($J=2k+4\beta S$) which predicts two competing contributions to the resulting exchange coupling. The first contribution corresponding to the exchange integral k (>0) is of ferromagnetic character, whereas the second contribution, proportional to the resonance integral β (<0) and the overlap integral S is antiferromagnetic. This model provides an argument for a sizable antiferromagnetic interaction for the d_{xy}, d_{xz} orbitals ($2k<<|4\beta S|$) and a weak antiferromagnetic interaction for the remaining d_{yz} orbital ($2k<|4\beta S|$). Let us denote the corresponding averaged contribution to the total exchange coupling by J_{AF}. The d_{z2} and d_{x2-y2} orbitals (e_g orbitals) of the M^{II} ion have zero overlap integrals and each results in an averaged ferromagnetic contribution J_F to the total

exchange coupling. The total exchange integral in the Nb^{IV}-CN-M^{II} unit can be expressed by the well known Kahn formula [5]:

$$J = \frac{1}{n_A n_B} \sum_{\mu=1}^{n_A} \sum_{\nu=1}^{n_B} J_{\mu\nu} \quad (4)$$

In equation (4) the A site corresponds to the Nb^{IV} ion and the B site to the M^{II} ion. Because there is only one electron on the $4d_{x2-y2}$ orbital of the Nb^{IV} center, we have always $n_{Nb} = 1$. The situation is case-dependent for the M^{II} center. Let us start with the analysis for **1** where M = Mn. The electronic configuration of Mn^{II} is $(t_{2g})^3(e_g)^2$, so there are five singly-occupied orbitals ($n_{Mn} = 5$). Hence for J_{MnNb} we obtain $J_{MnNb} = 1/5(3J_{AF} + 2J_F)$. This expression alone is insufficient to estimate both contributions from the subsequent pathways. We apply the same formula for compound **2** with M = Fe and the electronic configuration $(t_{2g})^4(e_g)^2$, which implies $n_{Fe} = 4$. Hence, the expression for the exchange coupling constant has the following form $J_{FeNb} = 1/4(2J_{AF} + 2J_F)$. Using J_{MnNb} and J_{FeNb} obtained from respective molecular field models one finds $J_{AF} = -21.6$ cm^{-1}, $J_F = +15.4$ cm^{-1}. Using these values one can calculate analogously the exchange couplings for the two remaining compounds. The electronic configuration of the Co^{II} ion in **3** is $(t_{2g})^5(e_g)^2$ and in this case $n_{Co} = 3$, and consequently $J_{CoNb} = 1/3(J_{AF} + 2J_F) = +3.1$ cm^{-1}. For **4** with M = Ni the corresponding electronic configuration is $(t_{2g})^6(e_g)^2$. The number of unpaired electrons is again reduced by 1, hence $n_{Ni} = 2$. The exchange coupling constant is given by $J_{NiNb} = 1/2(2J_F) = J_F = +15.4$ cm^{-1}. These values compare well with those of $J_{CoNb} = +3.5$ cm^{-1} and $J_{NiNb} = +8.1$ cm^{-1} estimated within the corresponding mean-field models.

5. Conclusions

Two approaches based on the mean-field approximation were taken to get insight into the exchange couplings in four isostructural compounds $\{[M^{II}(pyrazole)_4]_2[Nb^{IV}(CN)_8]\cdot 4H_2O\}_n$, where M^{II} = Mn, Fe, Co, Ni. The observed couplings were discussed using the simple-counting model (4) proposed by Kahn. This interpretation allows to predict the strength of exchange coupling for not yet reported Cr^{II} and V^{II} analogues of the $\{[M^{II}(pyrazole)_4]_2[Nb^{IV}(CN)_8]\cdot 4H_2O\}_n$ series: $J_{CrNb} = 1/4(3J_{AF} + J_F) \approx -12$ cm^{-1} and $J_{VNb} = 1/3(3J_{AF}) \approx -21$ cm^{-1}.

Acknowledgments

This work has been partially supported by the Polish Ministry of Science and Higher Education within Research Projects 0087/B/H03/2008/34 and 1535/B/H03/2009/36.

References

[1] Miller J S, Calabrese J C, Epstein A J, Bigelow R B, Zang J H and Reiff W M 1986 *J. Chem. Soc.: Chem. Commun.* 1026–28; Pei Y, Verdaguer M, Kahn O, Sletten J and Renard J P 1986 *J. Am. Chem. Soc.***108** 7428–30
[2] Yakhmi J V 2009 *Bull. Mater. Sci.* **32** 217–25; Férey G 2008 *Chem. Soc. Rev.* **37** 191–214
[3] Sieklucka B, Podgajny R, Przychodzeń P and Korzeniak T 2003 *Coord. Chem. Rev.* **249** 2203–21; Przychodzeń P, Korzeniak T, Podgajny R and Sieklucka B 2006 *Coord. Chem. Rev.* **250** 2234–60
[4] Pinkowicz D, Pełka R, Drath O, Nitek W, Bałanda M, Majcher A M, Poneti G and Sieklucka B 2010 *Inorg. Chem.* **49** 7565–76
[5] Kahn O 1993 *Molecular Magnetism* (New York: VCH Publishers, Inc.)
[6] Ohkoshi S I, Iyoda T, Fujishima A and Hashimoto K 1997 *Phys. Rev.* B **56** 11642–652
[7] Arai M, Kosaka W, Matsuda T and Ohkoshi S I 2008 *Angew. Chem. Int. Ed.* **47** 6885–87
[8] Kettle S F A 1996 *Physical Inorganic Chemistry. A Coordination Chemistry Approach* (Oxford: Oxford University Press)
[9] Abragam A and Bleaney B 1970 *Electron Paramagnetic Resonance of Transition Ions* (Oxford: Clarendon Press)
[10] Burdett J K, Hoffmann R and Fay R C 1978 *Inorg. Chem.* **17** 2553–68

Octacyanoniobate(IV)-based molecular magnets revealing 3D long-range order